J. Phys.: Condens. Matter **9** (1997) 3559–3573. Printed in the UK PII: S0953-8984(97)77380-6

Semi-empirical supercell calculations for free- and bound-hole polarons in α-Al_2O_3 crystal

Yu F Zhukovskii†‡, A A Sokol§, E A Kotomin†‖, C R A Catlow§ and R M Nieminen‡

† Institute of Solid State Physics, University of Latvia, 8 Kengaraga, LV-1063 Riga, Latvia
‡ Laboratory of Physics, Helsinki University of Technology, 1 Otakaari, FIN-02150 Espoo, Finland
§ The Royal Institution of Great Britain, 21 Albemarle Street, London W1X 4BS, UK
‖ Institute of Physics & Astronomy, Aarhus University, DK-8000 Aarhus-C, Denmark

Received 27 August 1996, in final form 13 December 1996

Abstract. Two different parametrizations of the semi-empirical method of the intermediate neglect of the differential overlap (INDO) are applied to the calculations of the small-radius hole polarons in the corundum (α-Al_2O_3) crystal. The 80-atom supercell has been used for the study of the atomic and electronic structure of a free small-radius hole polaron (the self-trapped hole, STH) and a hole polaron bound by a Mg impurity (the so-called V_{Mg} centre), respectively. Both parametrizations indicate that the two-site (quasi-molecular) configurations of both kinds of polaron have the lowest energy (which does not exclude the existence of one-site polarons also characterized by considerable relaxation energies). For V_{Mg} centres the lower energy is calculated for the defect configuration where the Mg-ion substitution is nearest to the hole polaron. Experimental ENDOR data on V_{Mg} defects are discussed in the light of the calculations.

1. Introduction

Corundum (α-Al_2O_3) is probably the most technologically important ceramic material, which has stimulated numerous studies of its optical and radiation properties [1–3]. However, only a few attempts have been made to understand theoretically the geometry and electronic structure of electron and hole defects in this material. This is due primarily to the complicated crystal structure of corundum and the partly covalent character of the chemical bonding. The semi-empirical quantum chemical method of intermediate neglect of the differential overlap (INDO) has been widely applied previously to point defects in a number of both ionic and partly ionic crystals, including several oxides [4–6]. This method [7] allows one to construct 'defect-containing' clusters comprising several tens or even hundreds of atoms and to carry out automated geometry relaxation around the defects using the relevant computer codes CLUSTERD [8] and SYM-SYM [9].

Recently, we applied the INDO method for *cluster* calculations of the basic defects in corundum. Results for a family of hole centres have already been published [4, 6, 10] along with a study of the electron centres—intrinsic F^+ and F defects (one or two electrons trapped by a single O vacancy, respectively) [11], centres associated with the Mg impurity (F_{Mg} and F^-_{Mg} defects in which a Mg^{2+} ion substitutes for Al^{3+} near to an F^+ or F centre) [12], and dimer (F_2-type) centres [13]. The 65-atom stoichiometric quantum cluster $Al_{26}O_{39}$

0953-8984/97/173559+15$19.50 © 1997 IOP Publishing Ltd

was used for these defect studies, this cluster being embedded into the electrostatic field of the rest of the crystal.

In this paper, we have used a new INDO parametrization for Al atoms based on structural and electronic properties of various simple aluminium-containing molecules and the perfect corundum crystal as well as improved two-centre parameters for O and Mg based on the corresponding properties of both MgO and corundum crystals (subsection 2.1). The use of the second parameter set allowed us to check that the earlier results are not an artefact of the parametrization developed in references [4, 8]. The reliability of the results could also be influenced by the electrostatic boundary conditions imposed on a cluster in the previous polaron calculations. To check this effect, we use here an 80-atom *supercell model* (subsection 2.2). As a test system we study the small-radius, hole polaron (the self-trapped hole, STH) in pure corundum [4, 6] and the hole polaron bound at the Mg impurity (the so-called V_{Mg} centre) [10]; both were studied earlier in the cluster model.

Bearing in mind the limitations of our semi-empirical calculations we focus more on a qualitative estimate of the stable configurations for the above-mentioned hole polarons in corundum. We believe that owing to a thorough optimization of the corresponding supercell structures, the results reported in this paper (section 3) are final for the semi-empirical level of theory. We will use them in our further investigation on the same system with *ab initio* methods.

2. Theoretical method

2.1. The modified INDO parametrization

The semi-empirical SCF calculation scheme in the INDO approximation, modified for simulations of point defects in the crystalline, essentially ionic systems under study was described in detail elsewhere [7, 8]. We recall here only that the construction of the Fock matrix is determined by the following set of both one- and two-centre empirical parameters for various types of valence *atomic orbital* (AO):

(i) the orbital exponent ζ_μ^A describing the radial part of the μth Slater-type AO on the A-atom;

(ii) the electronegativity of the A-atom $(E_{neg})_\mu^A$, defining the μth AO energy;

(iii) the μth AO population $(P^{(0)})_{\mu\mu}^A$, i.e. the 'initial guess' for the diagonal element of the density matrix;

(iv) the resonance integral $\beta_{\mu\nu}^{AB}$ entering the off-diagonal Fock matrix element where the μth and νth AOs are centred at the different A- and B-atoms; and

(v) the adjustable exponent α_μ^{AB} characterizing the extended nature of the B-atom core interaction with the electron localized on the μth AO of the A-atom.

The quality of these INDO parameters and steps that could be taken to improve them are of great importance. However, their choice is not a simple straightforward procedure but a result of a complicated search, aimed at reproducing reasonably well various features of molecules and crystals based on both experimental measurements and *ab initio* calculations.

By their very nature, semi-empirical methods are interpolative, and hence our primary concern is to choose an appropriate set of reference molecules and crystals. Since we study various point defects in corundum, we have used a number of small Al_mO_n molecules ($m = 1$–2 and $n = 0$–3) as well as the perfect corundum crystal itself to obtain a new parameter set. Such a choice provides us with different quantum states, bonding characters and effective charges that occur in real materials under various conditions. The parameter

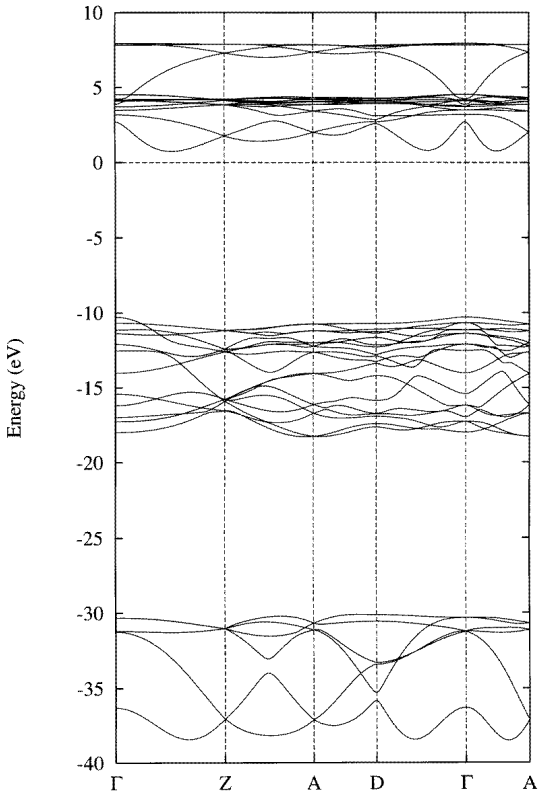

Figure 1. The band structure of corundum calculated along the symmetrical directions in the Brillouin zone. The designation of the special points is as follows: $\Gamma \equiv (0, 0, 0)$, $Z \equiv (\frac{1}{2}, \frac{1}{2}, \frac{1}{2})$, $A \equiv (0, \frac{1}{2}, 0)$, $D \equiv (\frac{1}{2}, \frac{1}{2}, 0)$.

set derived has been tested on a number of ternary compounds in order to estimate the overall error inherent in the semi-empirical scheme. For the perfect-corundum calculations, we used the periodic model in the form of the so-called *large unit cell* (LUC) including an integer number of primitive unit cells (UCs) [14]. The basic idea of this model is to perform an electronic structure calculation on the extended UC at the wave vector $\boldsymbol{k}' = \mathbf{0}$ in the narrowed Brillouin zone (NBZ), which is equivalent to a band calculation at several special $\boldsymbol{k}$-points of the BZ, for instance Γ, Z, A and D (figure 1), transforming to the NBZ centre after the corresponding extension of the primitive unit cell.

The previous ('old') INDO parametrization used for simulations of the various types of defect in corundum [4, 6, 10–13] led to some artefacts. For example, the lattice constant optimized for the 10-atom LUC was 5% smaller than the experimental value [4], but for the 80-atom LUC this difference approached 10%. Moreover, our intention is to obtain a description that is generally transferable to Al-containing oxides, hydroxides, and chlorides because the previous set of parameters has not allowed us to achieve this goal. For instance, the effective charges calculated earlier for the corresponding small molecules were quite similar to those obtained by the Mulliken analysis in *ab initio* calculations [15, 16]. However, this is in contrast to our previous experience that charge analyses performed in the neglect of differential overlap (NDO) approximations (originating from Pople's studies)

Table 1. The two INDO one-centre parameter sets used in the present supercell polaron simulations.

Type of element	AO	ζ (au^{-1})		E_{neg} (eV)		$P^{(0)}$ (e)		$-\beta$ (eV)	
		Old	New	Old	New	Old	New	Old	New
Al	3s	1.600	1.256	17.15	5.98	0.710	2.000	1.50	2.75
	3p	1.500	0.990	12.50	0.44	0.390	0.333	1.50	2.75
O	2s	2.270	2.270	4.50	4.50	1.974	1.974	16.00	16.00
	2p	1.860	1.860	−12.60	−12.60	1.960	1.960	16.00	16.00
Mg	3s	1.400	1.400	16.00	16.00	0.150	0.150	1.10	1.10

Table 2. The two INDO two-centre α-parameter (au^{-1}) sets used in the present supercell polaron simulations.

Type of element	Al		O		Mg	
	Old	New	Old	New	Old	New
Al	0.050	0.046	0.0	0.030	0.0	0.0
O	0.300	0.360	0.150	0.100	0.250	0.195
Mg	0.0	0.0	0.0	0.050	0.250	0.050

tend to yield essentially higher charges which are better compared to those from natural bond analysis [15]. The *effective charge* on the atom was determined here through a sum of diagonal elements of the density matrix in the AO representation:

$$q_A^{eff} = Z_A - \sum_{\mu}^{(A)} P_{\mu\mu} \tag{1}$$

where Z_A is the charge of the A-atom core (the wave function of the method is normalized in the standard NDO approximation). In the *Mulliken analysis* the charge on the A-atom is determined by the following formula:

$$q_A^{Mul} = Z_A - \sum_{\mu}^{(A)} \left(P_{\mu\mu} + \sum_{B(\neq A)} \sum_{\nu}^{(B)} P_{\mu\nu} S_{\mu\nu} \right) \tag{2}$$

where $S_{\mu\nu}$ is an overlap integral (q_A^{Mul} would correspond to q_A^{eff} if the normalization was the same). Overcoming these difficulties has led to a new set of parameters with two main features:

(i) the basis functions on Al are considerably more diffuse (the corresponding ζ-parameter has changed from 1.6 au^{-1} to 1.256 au^{-1} for 3s states, and from 1.5 au^{-1} to 0.99 au^{-1} for 3p states; see table 1);

(ii) the electron–core O–O interaction is much weaker than before (the α-parameter has dropped from 0.15 au^{-1} to 0.10 au^{-1}; see table 2).

As will be seen from the discussion below, the semi-empirical INDO scheme is based on a compromise between the quality of reproduction of a large number of compounds, with a particular emphasis on the structural and electronic properties. The primary goal of our new parametrization is the reliable reproduction of the ground-state *geometry* of pure and defect-containing corundum in the spirit of an NDO-type parametrization such as CNDO/BW or MINDO/3.

Table 3. The reference set of some small Al_mO_n molecules used for the fitting of INDO parameters. (Numbers in parentheses are a compilation of available experimental data and *ab initio* calculations.)

Type of molecule	Bond length (Å)		Atomization energy (eV)	Effective charge on Al (e)	Mulliken charge on Al (e)
Al_2	Al–Al	2.43 (2.43)	1.54 (1.55)	0.0	0.0
AlO	Al–O	1.64 (1.62)	7.60 (5.26)	1.0442	0.8822
AlO_2 (linear)	Al–O	1.70 (1.69)	14.07 (?)	2.0315	1.6927
Al_2O (linear)	Al–O	1.62 (1.73)	11.58 (10.67)	0.6999	0.5186
Al_2O_2	Al–O	1.75 (1.78)			
(D_{2h}, square)			22.38 (16.62)	1.3973	1.1060
	O–O	2.61 (2.62)			
Al_2O_2	Al–O	1.77 (1.95)			
(D_{2h}, rhombohedral)			23.28 (≈13.6)	0.8753	0.6796
	O–O	1.34 (1.62)			
Al_2O_3	$Al–O_{(1)}$	1.68 (1.69)			
(linear)			32.47 (19.7)	2.2182	1.8377
	$Al–O_{(2)}$	1.59 (1.63)			
Al_2O_3	Al–O	1.77 (1.77)			
(D_{3h}, bipyramidal)			34.60	2.2574	1.7663
	O–O	2.26 (2.52)			

Table 4. The dependence of corundum properties on the LUC size (the experimental corundum structure [19] is used).

UC extension	Total energy per primitive UC (au)	Effective charge on Al (e)	Valence band width (eV)	Band gap (eV)
$1 \times 1 \times 1$	−104.618 89	2.581	6.838	13.791
$2 \times 2 \times 2$	−105.484 14	2.408	7.211	12.289
$3 \times 3 \times 3$	−105.530 53	2.404	7.086	11.666
$4 \times 4 \times 4$	−105.530 14	2.404	7.238	11.679
$5 \times 5 \times 5$	−105.530 13	2.404	7.173	11.755

The results obtained for the reference set of molecules are summarized in table 3. We see that we generally calculate Al–O bond distances that are in good agreement with experiment or the results of *ab initio* calculations. We do, however, encounter certain problems in the case of bond angles (as observed in both Al_2O_2 and Al_2O_3 molecules); we attribute this problem to exaggerated O–O interactions. Moreover, we can confirm this conclusion from the trend in atomization energies—the more oxygen ions present in a molecule, the more exaggerated the predicted energy.

Two molecules presented in table 3 deserve further comment. In contrast to earlier calculations, the Al_2O molecule was found to be linear in all recent *ab initio* calculations [15, 16]. Presumably, the equilibrium angle of 144° previously reported is an artefact of the small basis sets used. With the new parameter set we find that the linear structure does indeed have a true minimum (whereas the previous set of INDO parameters gave a bent molecule). *Ab initio* calculations predict the bipyramidal form of Al_2O_3 to be stable only on the Hartree–Fock (HF) potential energy surface (the result being obtained using the GAUSSIAN 94 code with the 6-311G* basis set) [17]. Both MP2 [15] and our density functional (DFT) calculations performed by the BLYP/DNP method [18] yield a solution

with broken symmetry. (The closest local minimum has C_{2v} symmetry.) Nevertheless, we retain this molecule in the reference set because the bipyramidal configuration of the Al_2O_3 molecule represents the *structural formula unit* in the corundum crystal where the Madelung field is responsible for preserving the higher symmetry. Thus, one finds in table 3 for this particular molecule a comparison carried out only for the structural parameters and not for the atomization energy. The latter, available only at the Hartree–Fock level, is not of high enough quality to be used in our parametrization.

Calculations on all of the crystals described in this section have been done in the above-mentioned LUC model as implemented in the INDO code SYM-SYM [9]. The size of the LUC determines the quality of the calculation. In table 4 we have collected together data on the convergence of the electronic structure parameters with respect to the LUC size. (All of the calculations used here have been performed using the experimental structure of corundum.) The primitive unit cell of corundum contains two formula units; thus the number of atoms in the LUCs considered varies from 10 (the UC, or the LUC of a $1 \times 1 \times 1$ extension along the three translational vectors of the crystal) to 1250 (the LUC of a $5 \times 5 \times 5$ extension). From both our own experience and the data presented here we found that the *optimal* LUC size for use in corundum geometry optimization is $3 \times 3 \times 3$. Indeed, the total energy has practically converged for this LUC, whereas the charge density undergoes only minor changes comparing a LUC of $3 \times 3 \times 3$ and larger extensions. However, the parameters for the one-electron spectrum, although evaluated with an accuracy of about 2–3%, still require more extensive calculations. Finally, we carried out geometry optimization using two LUC sizes, of $2 \times 2 \times 2$ and $3 \times 3 \times 3$, and found that the difference in structural parameters for these two cases is less than 1%. Therefore, we can expect that a further extension of the LUC beyond $3 \times 3 \times 3$ will not yield any discernible changes in geometry.

Table 5. Optimized parameters of the corundum structure compared to experiment [19].

Structural parameter	Optimized value	Relative error (%)*
Rib of rhombohedral unit cell (a)	4.903 Å	4.4 (−)
Angle of rhombohedral unit cell (α)	59.5°	7.6 (+)
Volume of rhombohedral unit cell (V)	82.4 Å^3	3.0 (−)
Distance between nearest atoms (R^{NN}_{Al-O})	1.859 Å	0.1 (+)
Distance between next-nearest atoms (R^{NNN}_{O-O})	1.955 Å	0.7 (−)
Shortest distance between O atoms ($R^{(min)}_{O-O}$)	2.430 Å	4.0 (−)
Interbond angle in Al_2O_3 formula unit ($\angle$Al–O–Al)	93.67°	5.4 (−)

*Signs in parentheses indicate the direction of deviation from the experimental value.

Global optimization of the corundum crystal structure has given us the results presented in table 5. Again, the largest error is due to an exaggerated O–O interaction. Hence, the O–O distances and Al–O–Al bond angles are underestimated. However, the Al–O bond distances are in perfect agreement with the experiment, and because of error compensation the overall error for the unit-cell volume is only about 3%.

The band structure calculated for the optimized corundum crystal (figures 1 and 2) demonstrates the same general features as its *ab initio* counterparts (HF [20] and DFT [21] calculations): three flat, well separated bands, generated in turns by O 2s, 2p and Al hybridized 3sp states. All calculations predict an indirect band gap—that is, the lowest interband transition is not to the Γ point in the conduction band. In our study the dispersion curve at the bottom of the conduction band goes through a maximum at the Γ point,

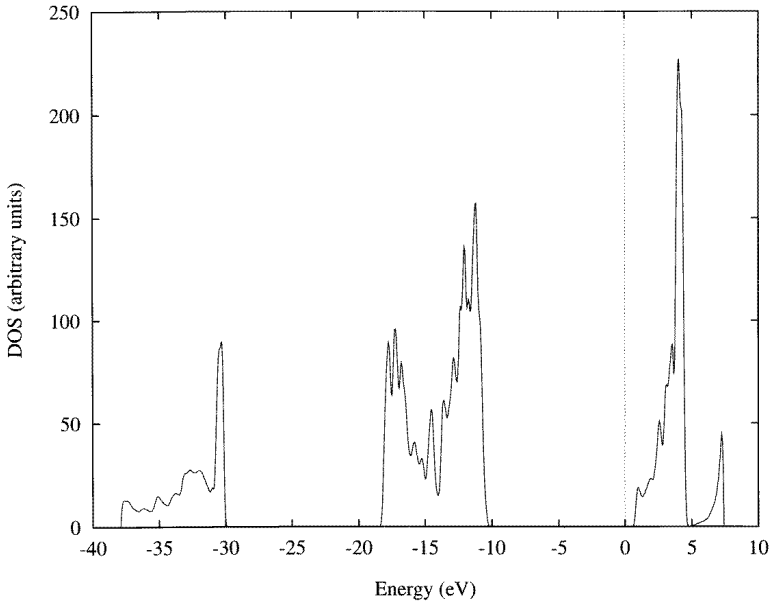

Figure 2. The calculated density of the electronic states in corundum. The original density of states has been calculated using a $7 \times 7 \times 7$ division of the Brillouin zone and then convoluted with a Gaussian curve having the dispersion 0.1 eV.

Table 6. Basic corundum properties obtained by various methods. (The theoretical data are calculated for the optimized corundum structure.)

Method	Upper valence band width (eV)	Band gap (eV)	Effective charge on Al (e)	Mulliken charge on Al (e)
This work	7.8	11.2	2.40	1.41
HF [20]	8.5	16.0		1.78
DFT [21]	7.4	6.3	2.63–2.75	
Experiment	9.3 [22]	9.5 [1]	1.32 [23]	1.32 [23]

whereas *ab initio* calculations predict it to be close to the minimum [20]. Moreover, our calculations give the bottom of the conduction band as consisting of Al 3p AOs which also contradicts both *ab initio* calculations as well as our previous data obtained using the earlier parametrization. These shortcomings of the new parameter set are probably the most serious and should be dealt with in future studies of excited states of crystals and their defects.

As follows from table 6, the main band parameters for the one-electron spectrum calculated here are intermediate between those obtained by *ab initio* HF and DFT approaches. Similar behaviour has also been found in many applications [4, 6]. Usually it is related to the fact that the local correlation effects can be partially taken into account in the semi-empirical schemes through parameters fitted to the experimental observables or to *ab initio* calculations that include the electron correlation. The effective charges calculated support the ionic character of the bonding in corundum; a comparison with the DFT results suggests that our charges are still somewhat underestimated but are closer to those experimentally estimated [23]. Mulliken charges predicted by *ab initio* HF calculations

[20] are also larger than in the present calculation. However, it is known that the Mulliken analysis underestimates effective charges when using Slater-type AOs even more than when using Gaussian orbitals.

Table 7. Unit-cell volumes calculated for corundum-related crystals.

Type of crystal	$AlNaO_2$ (alpha)	$MgAl_2O_4$ (spinel)	Al_2SiO_5 (andalusite)	$AlCl_3$	$AlNaCl_4$	AlOCl
Relative error, δV (%)	2.1	0.1	1.2	2.0	1.5	3.7

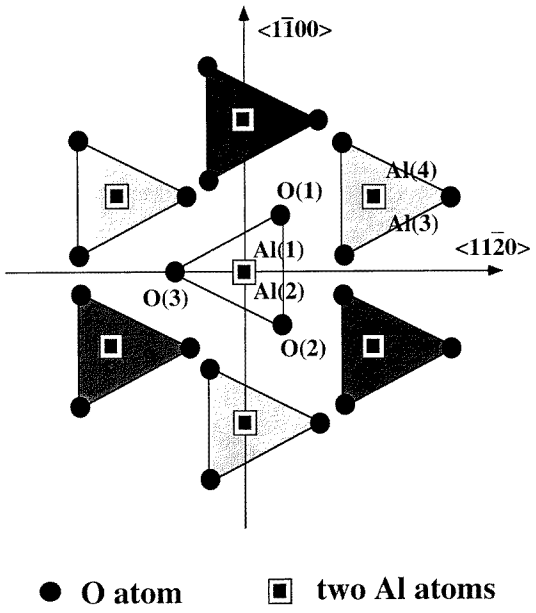

Figure 3. The projection of a 35-atom fragment of an 80-atom corundum $2 \times 2 \times 2$ supercell containing seven nearest Al_2O_3 formula units onto the (0001) plane (in order to simulate NNN or NN types of V_{Mg} defect either Al(1) or Al(4) atoms were replaced by Mg atoms, respectively). Such a fragment consists of three basal O planes shown in white, light grey (2.17 Å below the plane of the figure) and dark grey (2.17 Å above the plane). For all of the defect models, a two-site hole is shared by the O(1) and O(2) atoms, whereas the one-site hole is localized on the O(3) atom.

In contrast to the structural parameters, experimental data and the corresponding *ab initio* calculations on the electronic structure of *solid ternary compounds* are scarce. The relevant results of our calculations together with detailed analyses will be presented elsewhere. Here we plot only structural data for a number of crystals containing Al, O, and Cl atoms (table 7). Most are reproduced reasonably well using the set of parameters derived. The largest error is apparently mostly due to the poor quality of the O–O interaction parameters for these compounds. Nevertheless, an optimization of both MgO and spinel ($MgAl_2O_4$) crystals using the new INDO parametrization allowed us to improve also the two-centre parameters for Mg–O and Mg–Mg bonds in comparison with the old parameter set [8] (table 2). The results of semi-empirical calculations obtained for these crystals proved to be reasonable.

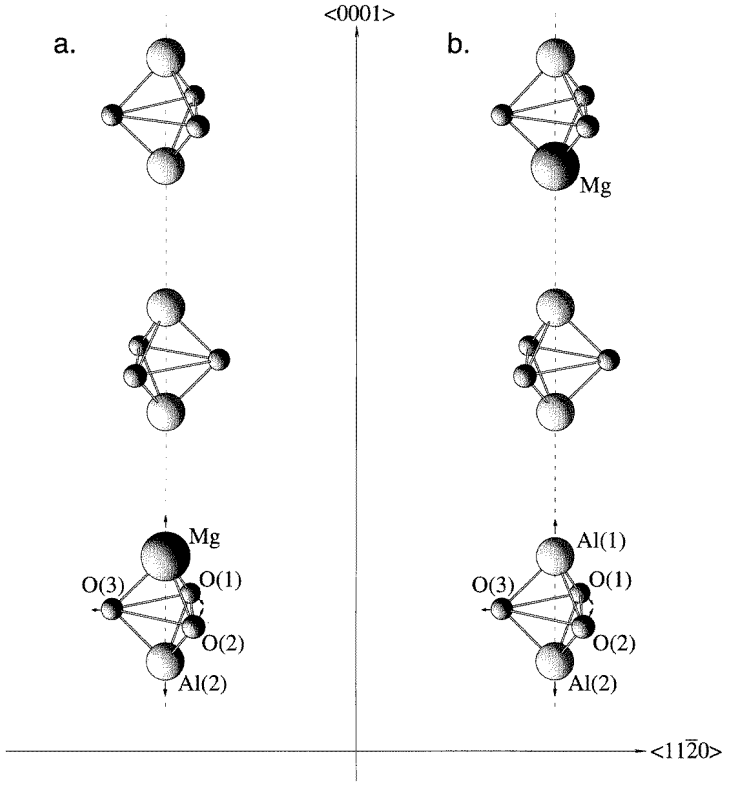

Figure 4. 15-atom fragments of the 80-atom corundum $2 \times 2 \times 2$ supercell containing three Al_2O_3 formula units (two adjacent units form the primitive unit cell Al_4O_6) where a Mg atom replaces a regular Al atom simulating both the NNN type of V_{Mg} defect (a) and the STH (b). In these two models a hole is either shared by the O(1) and O(2) atoms (the quasi-molecular polaron) or localized on the O(3) atom (the one-site polaron). The main directions for the atom displacements during structure relaxation are indicated by arrows.

In the next section we compare results from old and new parameter sets in our INDO calculations on polarons in the corundum crystal. The two sets of parameters summarized in tables 1 and 2 reveal a marked difference between all of the corresponding Al parameters. These calculations have been performed using the CLUSTERD code [8] considering the two-centre $\beta_{\mu\nu}$-parameters as the weighted values of diagonal elements of the resonance integral matrix, $\frac{1}{2}(\beta_{\mu\mu} + \beta_{\nu\nu})$; therefore these are presented in table 1 as one-centre parameters. We also note that none of the two-centre α-parameters in this scheme depends on the type of AO (table 2). The valence basis set in both parametrizations includes 3s and 3p AOs on Al atoms, 2s and 2p AOs on O atoms, and 3s AOs on Mg atoms.

2.2. The supercell (SC) model

We used the 80-atom $2 \times 2 \times 2$ supercell $Al_{32}O_{48}$ to study hole defects in corundum (figures 3 to 5). Such a supercell may be constructed by extension of a single 10-atom UC (the two upper formula units in figure 4(a)) by a factor of two along the three translational vectors. Each Al atom in a perfect corundum structure is surrounded by a distorted octahedron of O atoms forming two kinds of Al–O bond (table 5): 1.89 Å (in which the oxygen atom is the

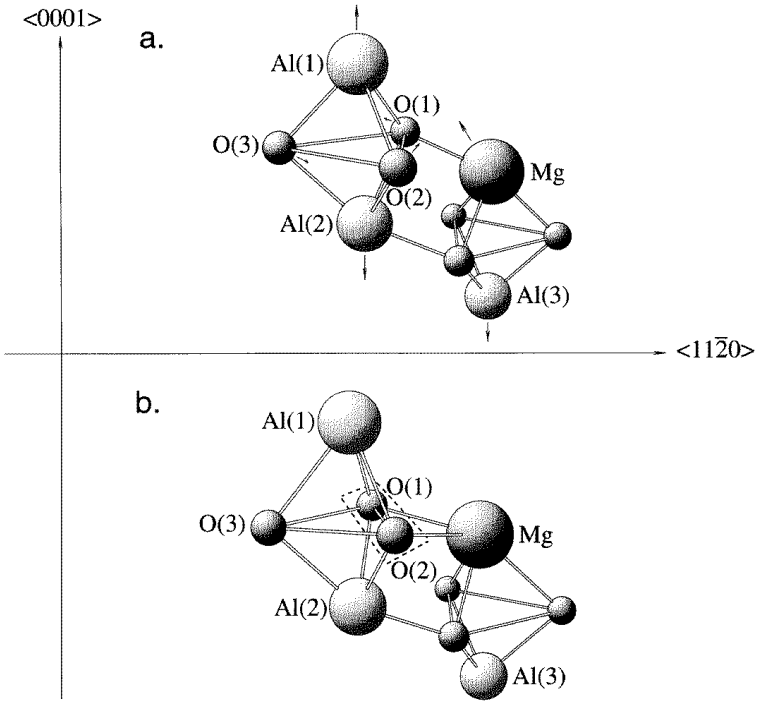

Figure 5. 10-atom fragments of the 80-atom corundum $2 \times 2 \times 2$ supercell containing two Al_2O_3 formula units from the adjacent UC where the Al atom from a neighbouring (lower) Al_2O_3 unit is replaced by a Mg atom, in order to simulate the NN type of V_{Mg} defect ((a) initial, unrelaxed structure, (b) relaxed structure). The two-site hole is shared by the O(1) and O(2) atoms; the marked region corresponds to ≈90% spin-density localization. Arrows indicate the main directions for the atom displacements during structure relaxation.

nearest neighbour, NN, to the Al atom) and 1.93 Å (where O is the next-nearest neighbour, NNN, to Al). In turn, each O atom is surrounded by four Al atoms, in two groups of two each at these distances. Obviously, every Al_2O_3 formula unit contains only the NNN Al–O bonds; NN bonds are formed by neighbouring Al and O atoms belonging to the nearest, but not the same UC (figure 5(a)). For instance, O(1), O(2), and O(3) atoms of the basic oxygen triangle arranged in the centre of a 35-atom fragment of the corundum $2 \times 2 \times 2$ supercell have six NN Al atoms from the adjacent formula units (figure 3): three upper Al atoms belonging to the 'light-grey' units, including the Al(4) atom, and three lower Al atoms from 'dark-grey' units. Obviously, the only NNN for these three oxygen atoms are Al(1) and Al(2) atoms. For the simulations of both STH and V_{Mg} centres, one of the Al atoms in this model has been substituted for with a Mg atom (figures 3 to 5).

An automated procedure for the atomic relaxation within the $2 \times 2 \times 2$ SC has been used for the simulation of various configurations of free- and bound-hole polarons in the corundum crystal. STH defects have been simulated by the substitution of a Mg atom for an Al atom in each supercell (figure 4(b)) keeping the supercell neutral. (The distance between the STH region and the remote Mg atom is large enough to avoid a direct influence on the properties of the STH—in particular, the hole density distribution in the defect-containing region.) The first stage of this relaxation procedure included both a structural optimization

of the corresponding Al_2O_3 formula unit and a variation of the Mg position. As the next step, a relaxation of the adjacent formula units was also carried out. A similar procedure has been used for the simulation of the NNN V_{Mg} defects (figure 4(a)). The first stage of the simulation of the NN V_{Mg} defect included the geometry optimization for atoms O(1), O(2), and O(3) forming a basic oxygen triangle as well as for both NN Mg and NNN Al(1), Al(2) atoms (figure 5(a)). Continuation and completion of this procedure included also relaxation of all of the surrounding Al_2O_3 formula units (shown in 'grey' in figure 3). Simulating the defect in this way corresponds to the hypothetical two-stage process of the hole self-trapping [6]: localization of a free hole on one or two atoms in a perfect-crystal region as the first stage, and the subsequent relaxation of the lattice with accompanying electron redistribution in this local region as the second stage, until the self-trapped (ST) state is formed.

The stability of various hole defects in a crystal may be characterized by the sign and magnitude of the *relaxation energy*, E_{rel}. This is the gain in energy due to displacements of the lattice atoms induced by the net charge of the localized hole:

$$E_{rel} = E_{def} - E_{perf} \tag{3}$$

where E_{def} is the total energy of the SC for the fully relaxed hole state, and E_{perf} is the total energy of the relevant unrelaxed supercell (containing the defect). In table 8 the values of the relaxation energies and spin densities for the stable configurations of the STH and V_{Mg} defects corresponding to the local minima on the total energy surface are presented for both parametrizations.

Table 8. The main results of calculations on the supercell model of the STH and V_{Mg} defects in corundum obtained using both sets of INDO parameters (marked as 'old' and 'new' in tables 1 and 2).

Characteristics	Parameters	Two-centre STH defect	Various types of V_{Mg} defect		
			Two-centre NN	One-centre NNN	Two-centre NNN
$\lvert E_{rel}\rvert$ (eV)*	Old	3.41	7.46	1.61	4.30
	New	1.43	4.03	1.26	2.31
Spin density (e)	Old	0.92 (0.45 + 0.47)	0.91 (0.44 + 0.47)	0.70	0.91 (0.45 + 0.46)
	New	0.89 (0.44 + 0.45)	0.90 (0.45 + 0.45)	0.72	0.88 (0.44 + 0.44)

*Since all relaxation energies are negative, their absolute values are given here.

3. Results and discussion

The use of our new parametrization adequately improves some of the results of the INDO calculations for the 80-atom supercell model of perfect crystalline corundum. The optimized lattice constant is now found to be only by 4.4% less than the experimental value (much better than the value of 10% for the old parameters). The one-electron gap decreased from 12.8 eV (with the old set of parameters) to 11.2 eV, and the width of the upper valence band changed similarly from 11.4 eV to 7.8 eV; in both cases the recalculated data are closer to the corresponding values determined experimentally (9.5 eV and 9.3 eV, respectively—see table 6). At the same time, the new parameters lead to an unrealistic description of the bottom of the conduction band (3p Al levels lie lower than 3s Al ones), so a study of the excited states as well as the optical transitions in corundum becomes rather problematic for the new parametrization.

The effective charges in the perfect crystal change insignificantly: 2.36 e ('old')/2.40 e ('new') for Al atoms as well as -1.57 e ('old')/-1.60 e ('new') for O atoms. They are close to those obtained in recent *ab initio* calculations (2.02 e on Al and -1.35 e on O) [20]. The Mulliken population analysis resulting from the old set of parameters shows that O–O bonds are almost unpopulated by electrons whereas both NN and NNN kinds of Al–O bond reveal rather high electron populations (0.26 e and 0.17 e, respectively); that is, these Al–O bonds are directly responsible for the partially covalent nature of the chemical bonding in corundum.

As is clear from table 8, the new set of parameters results in an appreciable decrease in the relaxation energies for all of the types of hole defect under study, whereas the spin density in the corresponding defect-containing regions either slightly increases (the one-site hole) or slightly decreases (the quasi-molecular hole). Obviously, the corresponding values of $|E_{rel}|$ are reduced due to much smaller binding energies of the O_2, O_2^-, and O_2^{2-} species as compared with the previous parametrization. Nevertheless, the set of *relative* structural parameters ($\Delta R_i/R_i$) and the electron density distribution $\rho(\boldsymbol{r})$ for the hole defects considered are similar for the two sets of parameters. Our subsequent discussion therefore concentrates on these properties.

3.1. STH centres

Both *one*-site (atomic) and *two*-site (quasi-molecular) free polarons were considered in our STH simulations. In contrast to our previous cluster calculations [4, 10], the supercell model indicates that the one-site STH centre localized on the O(3) atom (figure 4(b)) is unstable with respect to the transformation into the quasi-molecular configuration. We note that a cluster model predicted the existence of a local minimum at the potential energy surface corresponding to such a polaron, with $E_{rel} \approx 1.9$ eV [4]. A possible reason for this disagreement is the difference between the two models: unlike the supercell approximation described above, a positively charged stoichiometric cluster containing a few Al_2O_3 formula units was embedded into the electrostatic field of the rest of a perfect corundum lattice, thus neglecting bond breaking of the atoms at the cluster boundary.

The quasi-molecular model of the free polaron obtained in our calculations is very similar to that known for a long time as the V_K centre in alkali halides [24]. Its optimized geometry shows that two oxygen atoms, O(1) and O(2), are strongly relaxed inwards (≈40% of the O–O distance in a regular lattice) and that this is accompanied by an outward ≈20% displacement of both NNN Al(1) and Al(2) atoms on each side of the O triangle (figure 4(b)). The displacement vectors of these two O atoms form an angle of ≈20° with respect to the straight line connecting their perfect-lattice sites. The same configuration was predicted for a free three-atom molecule by the general Jahn–Teller theory. The supercell STH geometry is close to that of our previous cluster simulations [4, 6].

The main contribution to hole self-trapping comes from the linear relaxation of the *two* oxygen atoms, O(1) and O(2). These O atoms share about 90% of the hole density. A closer analysis of the origin of this strong localization shows that it arises from the chemical bonding between the two above-mentioned oxygen atoms O(1) and O(2): the population of their bond is close to that for the Al–O bond in the perfect crystal. Moreover, an automated atomic relaxation undertaken for the supercell model for both parametrizations reveals a rotation by ≈6° of the basic oxygen triangle O(1)–O(2)–O(3) with respect to the Al(1)–Al(2) axis. Such a rotation is accompanied by a simultaneous Mg-atom displacement from that axis, and is analogous to that observed for the off-centre impurities in ionic solids [25].

3.2. V_{Mg} centres

In the SC of bound-hole polarons (figures 4(a) and 5) the same spatial configurations as in the case of STHs were carefully studied and compared: the one-site V_{Mg} centre with a hole localized on a *single* O(3) atom, and the two-site V_{Mg} centre where a hole is shared by the *two* atoms, O(1) and O(2). These bound polarons could coexist (both values of E_{rel} are negative), and our calculations indicate a preference for the *two-site* configurations as the energetically most favourable. In the V_{Mg} centres a hole is partly trapped by a Mg atom having a smaller charge than the Al atom for which it substitutes; effectively Mg has a *negative* charge with respect to the perfect corundum lattice. In a purely ionic model its formal charge would be $-1\ e$. Apparently, this would also be the total charge of the whole centre. As regards our self-consistent calculations using the old parameter set, we obtained $q_{Mg} = 1.89\ e$ for the relevant unrelaxed SC, whereas for an Al atom in the perfect corundum, $q_{Al} = 2.36\ e$. Therefore the *effective* Mg charge is only $-0.47\ e$ while the remaining part of the hole density in the unrelaxed structure is shared by the neighbouring oxygen atoms. Thus, the V_{Mg} centre can be considered as a *perturbed* STH.

The *only* stable one-site V_{Mg} configuration is that where the Mg impurity is in the NNN cation position with respect to an O^- ion. The stable structural configuration of this defect is characterized, first of all, by a considerable displacement of the O(3) atom (figures 3 and 4(a)) towards the centre of the basic oxygen triangle. Hole localization on this atom has mainly an electrostatic origin, since this atom is essentially closer to the negatively charged Mg ion than that at the regular site. For the NN configuration of V_{Mg} centres, both parametrizations indicate *instability* of the one-site conformation

As regards the quasi-molecular configurations of the V_{Mg} defect, our calculations favour the Mg ion in the NN position rather than the NNN position (table 8). The equilibrium configuration for the *two*-site NN V_{Mg} centre is shown in figure 5(b). During the optimization procedure, atoms of the oxygen triangle O(1)–O(2)–O(3) are synchronously displaced along the two trajectories: they all rotate by $\approx 15^\circ$ with respect to the Al(1)–Al(2) axis, and simultaneously the O(1) and O(2) atoms relax towards each other (as in the case of the two-site STH). At the same time, the Mg atom shifts towards the basic oxygen triangle, from which the Al(1) and Al(2) atoms are displaced outwards. This represents the detailed optimization of the geometry of this defect.

The two-site NNN V_{Mg} centres (figure 4(a)) are similar to the analogous STH configuration described above. According to the old parametrization, the bond population between the O(1) and O(2) atoms sharing a hole is $\approx 0.3\ e$, i.e. slightly higher than in the STH case ($0.267\ e$). In turn, the Al–O bond population ($0.228\ e$) is reduced compared to that in the perfect corundum ($0.258\ e$). An automated optimization procedure for this configuration indicates also a rotation by $\approx 7^\circ$ of the basic oxygen triangle with respect to the Al(1)–Al(2) axis. We find a gain in the relaxation energy of ≈ 0.5 eV caused by both the rotation of the basic oxygen triangle and the displacement of all of the atoms of the basic Al_2O_3 unit from the positions of the symmetrical quasi-molecular configuration of the NNN V_{Mg} defect. However, due to the complex lattice structure of corundum we were unable to estimate the transition barrier between the NN and NNN configurations of V_{Mg} defects on a total energy surface.

V_{Mg} centres have been studied experimentally by means of ESR/ENDOR techniques [26] where only a *one-site* hole polaron was discovered. These studies give an experimental estimate of the defect geometry which greatly differs from our calculations. We found, however, that this 'experimental' geometry is even less favourable energetically than the perfect-crystal geometry: the relevant $E_{rel} \geqslant 0.3$ eV. There are several possible explanations

of our disagreement with these experimental results. First, only the relative distances between atoms could be extracted from ESR/ENDOR measurements; for example, it is not clear from [26] whether the Mg atom is displaced from a regular Al site and the O^- atom is in the plane containing the three nearest Al atoms (two of them lie below the basal O plane whereas the third one lies above it); moreover, it is also unclear whether Mg was present in significant concentrations in the samples or whether the hole was trapped by Al vacancies. Secondly, in these estimates any covalency in the corundum crystal was neglected. It would be of great interest to search for the theoretically predicted *two-site* V_{Mg} configuration. Probably, its observation by ENDOR is masked by the large number of lines in the relevant experimental spectrum for such a low-symmetry defect. In this respect, Raman scattering spectroscopy may be a more promising tool.

On the whole, energetic differences obtained by the INDO modelling remain questionable and should be the subject of further investigations at a better level of theory. We are working now on an *ab initio* approach to the problem of the lowest-energy configuration for the V_{Mg} centres in corundum.

We note, in conclusion, that the energetics of small-polaron formation in corundum is not a trivial problem. The possibility of the hole self-trapping in the form of a small-radius polaron localized by a single atom or two atoms (atomic versus molecular polarons) is determined by the sign of the self-trapping energy. This latter is a sum of three contributions: the positive localization energy E_{loc}, required for the localization of a Bloch-like wavepacket of the free, band hole on the atom or pair of atoms at the first stage of the self-trapping; and two negative contributions—due to chemical bonding (for molecular polarons, as in the present case) and the lattice polarization energy. The generally accepted simple estimate of E_{loc} (e.g., [27]) as the half-width of the upper valence band, E_w, renders the hole self-trapping hardly possible, since in corundum $E_w = 8$ eV. However, this estimate for E_{loc} is valid only for crystals with symmetric and smooth densities of the valence band states (DOS). This is not true for corundum with a strongly (O 2p–Al 3p) mixed valence band and a flat oxygen subband at the top of the total valence band. For such cases a novel formalism has been presented in [6]. Unlike previous model Hamiltonian approaches, it is based on the self-consistent quantum mechanical calculations of the band structure of real materials, incorporating the covalence effects in their chemical bonding. (The calculated effective charges differ strongly from those known from the commonly used ionic model: $+2.34\ e$ on Al and $-1.56\ e$ on O ions.) Application of this theory to corundum [6] has demonstrated that E_{loc} is significantly less than $\frac{1}{2}E_w$, which makes hole self-trapping energetically favourable. This shows that quantum mechanical simulation of the carrier self-trapping is a powerful tool for the realistic study of technologically important (rather than model) materials.

4. Conclusions

The two INDO parametrizations carefully compared in this paper agree that the only stable *one-site* configuration of the bound-hole polaron in corundum crystals is that where the Mg impurity is substituting for the next-nearest (NNN) Al atom. This simple result is in agreement with a previous experimental ESR/ENDOR study [26]. However, our calculations predict also the existence of another species, the *two-site* bound polaron (whose energy given by the semi-empirical method used is lower than that for the one-site polaron). Unlike the case for the one-site polaron, both parametrizations give preference to the nearest (NN) Mg ion substituting for an Al atom. The experimental search for such polarons, e.g. using Raman scattering, and further theoretical investigations are of great interest.

Acknowledgments

EK was supported by an EC HCM grant: 'Polarons, bipolarons and excitons: properties and occurrence in new materials' through contract No ERBCIPDCT94-0031. YZ is greatly indebted to the CIMO Foundation (Finland) for financial support, and to members of the Laboratory of Physics at Helsinki University of Technology for warm hospitality during his stay there. The calculations were performed using the computer facilities of both the Finnish Centre for Scientific Computing (CSC) and the Computing Centre of the Royal Institution (London) to whom we are also greatly indebted. The authors express their gratitude to J T Devreese, N Itoh, L N Kantorovich and A L Shluger for stimulating discussions.

References

[1] Valbis J and Itoh N 1991 *Radiat. Eff. Defects Solids* **116** 171
[2] Spaeth J-M and Koschnick F K 1991 *J. Phys. Chem. Solids* **52** 1
[3] Caulfield K J, Cooper R and Boad J F 1993 *Phys. Rev.* B **47** 55
[4] Jacobs P W M, Kotomin E A, Stashans A, Stefanovich E V and Tale I A 1992 *J. Phys.: Condens. Matter* **4** 7531
[5] Shluger A L and Stefanovich E V 1990 *Phys. Rev.* B **42** 9646
Shluger A L, Grimes R W, Catlow C R A and Itoh N 1991 *J. Phys.: Condens. Matter* **3** 8027
[6] Kantorovich L N, Stashans A, Kotomin E A and Jacobs P W M 1994 *Int. J. Quantum Chem.* **52** 1177
[7] Kotomin E A and Shluger A L 1982 *Phys. Status Solidi* b **109** 75
Shluger A L 1985 *Theor. Chim. Acta* **66** 355
Shluger A L and Itoh N 1990 *J. Phys.: Condens. Matter* **2** 4119
[8] Stefanovich E V, Shidlovskaya E K, Shluger A L and Zakharov M A 1990 *Phys. Status Solidi* b **160** 529
[9] Kantorovich L N and Lifshitz A I 1992 *Phys. Status Solidi* b **174** 79
Kantorovich L N and Lifshitz A I 1993 *SYM-SYM INDO Computer Code. User Guide* (Riga: University of Latvia Press)
[10] Jacobs P W M and Kotomin E A 1992 *Phys. Rev. Lett.* **69** 1411
Jacobs P W M, Kotomin E A, Stashans A and Tale I A 1993 *Phil. Mag.* B **67** 557
Jacobs P W M, Kotomin E A, Stashans A and Tale I A 1994 *Modell. Simul. Mater. Sci. Eng.* **2** 109
[11] Stashans A, Kotomin E A and Calais J-L 1994 *Phys. Rev.* B **49** 14 854
[12] Kotomin E A, Stashans A and Jacobs P W M 1995 *Radiat. Eff. Defects Solids* **134** 87
[13] Kotomin E A, Stashans A, Kantorovich L N, Lifshitz A I, Popov A I, Tale I A and Calais J-L 1995 *Phys. Rev.* B **51** 8770
[14] Evarestov R A and Lovchikov V A 1977 *Phys. Status Solidi* b **93** 469
Evarestov R A and Lovchikov V A 1979 *Phys. Status Solidi* b **97** 743
Evarestov R A 1982 *Quantum-Chemical Methods in Solid State Theory* (Leningrad: Leningrad State University Press)
[15] Nemukhin A V and Weinhold F 1992 *J. Phys. Chem.* **97** 3420
[16] Bencivenni L, Pelino M and Ramondo F 1992 *J. Mol. Struct.* **253** 109
[17] *GAUSSIAN 94* 1995 *Revision D1* (Pittsburgh, PA: Gaussian Inc.)
[18] *DMOL 95.0/3.0.0* 1995 *User Guide* (San Diego, CA: Biosym/MSI)
[19] Wyckoff R W G 1964 *Crystal Structures* 2nd edn, vol 2 (New York: Interscience) p 6
Bialas H and Stolz H J 1975 *Z. Phys.* B **21** 319
[20] Salasco L, Dovesi R, Orlando R, Causà M and Saunders V R 1991 *Mol. Phys.* **72** 267
[21] Xu Y N and Ching W Y 1991 *Phys. Rev.* B **43** 4461
Ching W Y and Xu Y N 1994 *J. Am. Ceram. Soc.* **77** 404
[22] O'Brien W L, Jia J, Dong Q-Y, Callcott T A, Miyano K E, Ederer D L, Mueller D R and Kao C-C 1993 *Phys. Rev.* B **47** 140
[23] Lewis J, Schwarzenbach D and Flack H D 1982 *Acta Crystallogr.* A **38** 733
[24] Kabler M N 1972 *Point Defects in Solids* ed J H Crawford and L M Slifkin (New York: Plenum) p 372
[25] Stoneham A M 1975 *Theory of Defects in Solids* (Oxford: Clarendon)
[26] DuVarney R C, Niklas J R and Spaeth J-M 1985 *Phys. Status Solidi* b **128** 673
Adrian F J, Nette A N and Spaeth J-M 1985 *Phys. Rev.* B **31** 3923
[27] Alexandrov A S and Mott N F 1996 *Polarons and Bipolarons* (Cambridge: World Scientific)